

Supplementary Information

**Factors affecting the electron-phonon coupling in FeSe under
pressure**

Tingting Li^{a, b}, Xiaoli Zhang^{a, b, *}, Zhi Zeng^{a, b, *}

^a Key Laboratory of Materials Physics, Institute of Solid State Physics, HFIPS, Chinese Academy of Sciences, Hefei 230031, China

^b Science Island Branch of Graduate School, University of Science and Technology of China, Hefei 230026, China

*Corresponding author

Email: xlzhang@theory.issp.ac.cn, zzeng@theory.issp.ac.cn

To ensure good convergencies, we test the phonon frequency convergencies with the changing k and q grids. First, we test the k grid convergence based on the ground state FeSe unit cell using $30 \times 30 \times 30$ and $32 \times 32 \times 32$ k grids. The phonon dispersions along the high symmetry lines are shown in Fig. S1(a), where the dashed blue and the solid red lines are related to the $30 \times 30 \times 30$ and $32 \times 32 \times 32$ k grids, respectively. The frequency difference along the high symmetry lines is less than 0.9 cm^{-1} , indicating that the convergence can be achieved by using the k grid larger than $30 \times 30 \times 30$. Therefore, we choose the $32 \times 32 \times 32$ k grids for phonon-related calculations of the ground state FeSe unit cell. Accordingly, the $16 \times 16 \times 16$ and the $11 \times 11 \times 11$ k grids are used for $2 \times 2 \times 2$ and $3 \times 3 \times 3$ supercells, respectively.

Then, we test the convergency of q by using the $1 \times 1 \times 1$, $2 \times 2 \times 2$ and $3 \times 3 \times 3$ supercells. The calculated phonon dispersions are shown in Fig. S1(b), where the solid gray and the solid red and dashed blue lines are related to the $1 \times 1 \times 1$ and $2 \times 2 \times 2$ and $3 \times 3 \times 3$ supercells, respectively. The frequency difference between the $1 \times 1 \times 1$ and $2 \times 2 \times 2$ supercells along the high-symmetry lines (see X- Γ and Γ -M) are obvious, whereas the frequency difference between the $2 \times 2 \times 2$ and $3 \times 3 \times 3$ supercells along the high-symmetry lines are much smaller, see Fig. S1(b). The frequency difference between the $2 \times 2 \times 2$ and $3 \times 3 \times 3$ supercells along the high symmetry lines is less than 19 cm^{-1} . In addition, we calculate the mean square displacements (MSD) of Fe and Se atoms by using the $1 \times 1 \times 1$, the $2 \times 2 \times 2$ and $3 \times 3 \times 3$ supercells. The results are shown in Fig. S1(c) and S1(d). The MSD refers to the deviation of the particle's position relative to the reference position under certain temperature, which relates directly to the displacements of atoms. The MSD (either for Fe or Se atom) for the $2 \times 2 \times 2$ supercell (the red lines) is close to that for $3 \times 3 \times 3$ supercell (the blue lines) but deviate a lot from that of the unit cell (the gray lines), as shown in Fig. S1(c) and S1(d). Thus, the phonon frequency together with the MSD tests show that the convergence is achieved by using the supercells larger than $2 \times 2 \times 2$. Therefore, we choose the $2 \times 2 \times 2$ q grids in phonon related calculations.

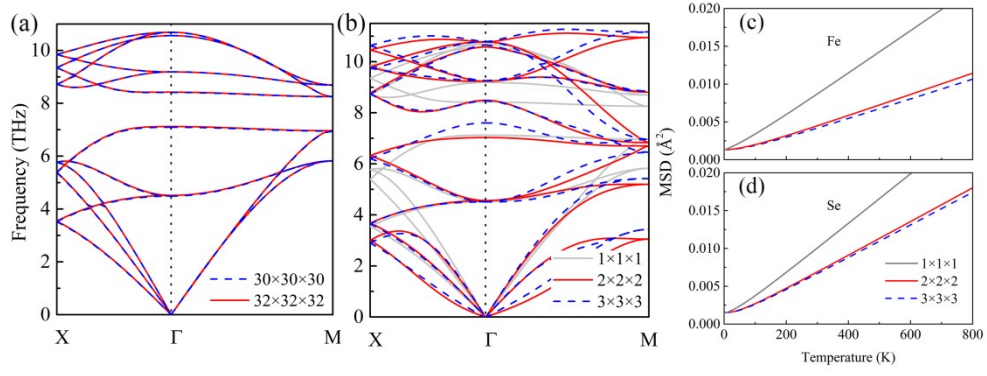


Figure S1: Phonon dispersion convergence tests respect to k and q grids. (a) The phonon dispersions of ground state FeSe unit cell using the $30 \times 30 \times 30$ (dashed blue lines) and $32 \times 32 \times 32$ (solid red lines) k grids. (b) The phonon dispersions of ground state FeSe using the $1 \times 1 \times 1$ (solid gray lines), the $2 \times 2 \times 2$ (solid red lines) and $3 \times 3 \times 3$ (dashed blue lines) supercells. The mean square displacements (MSD) of (c) Fe and (d) Se atoms as a function of temperature using the $1 \times 1 \times 1$ (solid gray lines), the $2 \times 2 \times 2$ (solid red lines) and the $3 \times 3 \times 3$ (dashed blue lines) supercells.

We present the partial density of states (PDOS) of ground state FeSe. Fig. S2(a) shows the PDOS of

ground state FeSe, where the states around the Fermi level are hybridized Fe and Se states with mainly Fe states. Fig. S2(b) shows the PDOS of Fe at the ground state and under three different pressure conditions. The Fe states around the Fermi level increase under hydrostatic pressure and the increased Wyckoff position z_{Se} , while decrease under the decreased lattice constants compared to that in the FeSe ground state structure. Fig. S2(c) shows the PDOS of Fe under the in-plane biaxial strain, where the Fe states around the Fermi level also increase compared to that in the FeSe ground state structure.

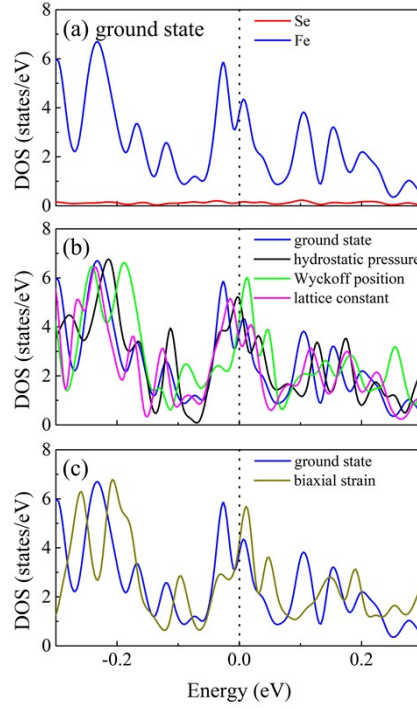


Figure S2: The PDOS of FeSe. (a) At the ground state, in which the blue and red lines represent the PDOS of Fe and Se, respectively. (b) The Fe PDOS under three different pressure conditions, in which the solid black, green, and magenta lines are related to hydrostatic pressure, increased Wyckoff position z_{Se} , decreased lattice constants, respectively. (c) The Fe PDOS under the in-plane -1.24% compressive biaxial strain. The black dash lines represent the Fermi level.

In the main text, we calculate the Poisson ratio thus the c lattice constant when applying an in-plane

biaxial strain. This method is commonly used in experiments. On the other hand, in the DFT studies, the c lattice constant can also be optimized while fixing the in-plane compressive a lattice constant. We calculated the relative physical properties based on the above two methods to see the difference.

The Fermi surfaces for structure from the calculation of Poisson ratio and DFT optimization under the in-plane 1.24% biaxial compressive strain are shown in Fig. S3 (a) and (b), respectively. Both of them have three hole pockets at the Γ point and two electron pockets at the M point as shown in Fig. S3(a) and S3(b). The $N(E_F)$ show slight difference with a value of 19.652 for structure with the calculation of Poisson ratio and 19.629 for the structure with DFT optimization. The Raman frequencies for the structure under either the calculation of Poisson ratio or DFT optimization show the same trend and slight quantitative difference, see Fig. S3(c). The electron-phonon coupling constant with DFT optimized structure is 0.270, which is larger than that of 0.214 with the calculation of Poisson ratio structure. Thus, using the DFT optimization structure, we get even larger electron-phonon coupling constant, which also indicate the in-plane biaxial compressive strain can increase the superconductivity of the FeSe. Therefore, the conclusion is the same as we got based on the calculation of Poisson ratio structure. The Eliashberg functions $\alpha^2F(\omega)$ with the integrated $\lambda(\omega)$ as a function of frequency are shown in Fig. S4. There is no much difference between these two Eliashberg functions, indicating either method will give the same conclusion.

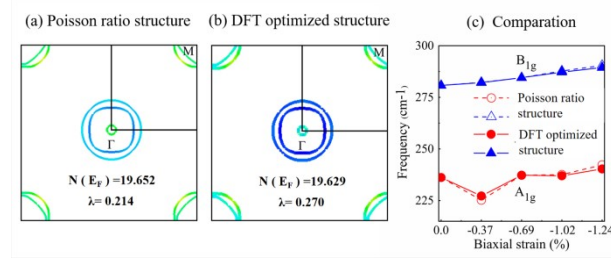


Figure S3: The Fermi surface and the Raman frequencies under the in-plane 1.24% biaxial compressive strain. The Fermi surface on the $k_z = 0$ of (a) the calculation of Poisson ratio structure and (b) the DFT optimized structure. (c) The A_{1g} and B_{1g} Raman frequencies. The dashed lines and solid lines represents the Poisson ratio and the DFT optimized structure, respectively.

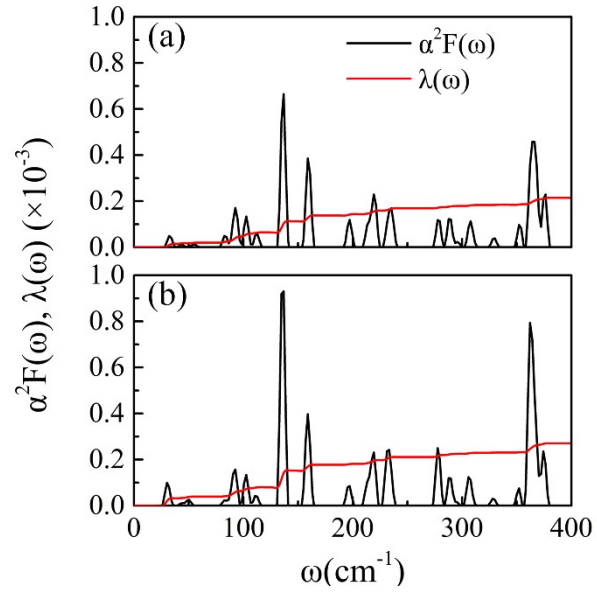


Figure S4: The Eliashberg functions $\alpha^2 F(\omega)$ and the integrated $\lambda(\omega)$ as a function of frequency of FeSe under the in-plane 1.24% biaxial compressive strain for (a) the calculation of Poisson ratio structure and (b) the DFT optimized structure.